

# Simple voltammetric approach for characterization of two-step surface electrode mechanism in protein-film voltammetry

Rubin Gulaboski<sup>1</sup> · Valentin Mirceski<sup>2,3</sup>Received: 13 March 2020 / Revised: 18 March 2020 / Accepted: 18 March 2020  
© Springer-Verlag GmbH Germany, part of Springer Nature 2020

## Abstract

Many enzymes embedding multivalent metal ions or quinone moieties as redox-active centres undergo electrochemical transformation via two successive electron transfer steps. If electrochemical features of such redox enzymes are analyzed with “protein-film voltammetry”, one frequently meets a challenging reaction scenario where the two electron transfers take place at the same formal potential. Under such conditions, one observes voltammogram with a single oxidation-reduction pattern hiding voltammetric features of both redox reactions. By exploring some aspects of the two-step surface EECrev mechanism one can develop simple methodology under conditions of square-wave voltammetry to enable recognizing and characterizing each electron transfer step. The method relies on the voltammetric features of the second electron transfer, which is coupled to a follow-up chemical reaction. The response of the second electron transfer step shifts to more positive potentials by increasing the rate of the chemical reaction. The proposed methodology can be experimentally applied by modifying the concentration of an electrochemically inactive substrate, which affects the rate of the follow-up chemical reaction. The final voltammetric output is represented by two well-separated square-wave voltammetric peaks that can be further exploited for complete thermodynamic and kinetic analysis of the EECrev mechanism.

**Keywords** Square-wave voltammetry · Two-step electrode mechanism · Kinetics of electron transfer · Protein-film voltammetry

## Introduction

Protein-film voltammetry is a valuable methodology introduced about two decades ago that enables an insight into important electrochemical and chemical features of many enzymes [1–5]. By adsorption of a given lipophilic enzyme on the surface of a working electrode one prepares an enzyme-modified electrode, which is suitable for exploration of protein

redox chemistry by means of a common three-electrode setup. Valuable data about mechanisms of action of many proteins, as well as important thermodynamic and kinetic parameters of the redox transformations of many enzymes, have been obtained in the last 20 years [1–5].

Many of the analyzed enzymes, in particular those featuring multivalent redox centres, exhibit rather complex electrochemical behaviour [1, 4, 5]. Such group can be exemplified with redox enzymes having quinone/hydroquinone moiety [6], or polyvalent cations of Mo, V, W or Mn [1, 3, 7–10] in the structure. Since many of these enzymes can undergo electrochemical transformation via successive exchange of electrons with the working electrode, their voltammetric patterns can be exceptionally complex [1–5]. As it is described in [11], their complex electrochemistry can be successfully resolved by square-wave voltammetry (SWV). In the theoretical models related to the two-step successive electrode mechanisms of [11–20], it has been recently reported on reliable procedures to characterize particular electrode enzymatic mechanism, in which coupled chemical steps occur. Moreover, relatively simple methodology has been elaborated

We dedicate this work on the occasion of the 65th birthday of our supervisor and great friend, professor Fritz Scholz.

✉ Rubin Gulaboski  
rubin.gulaboski@ugd.edu.mk

<sup>1</sup> Faculty of Medical Sciences, Goce Delcev University, Stip, Macedonia

<sup>2</sup> Department of Chemistry, Faculty of Natural Sciences and Mathematics, Ss Cyril and Methodius University, Skopje, Macedonia

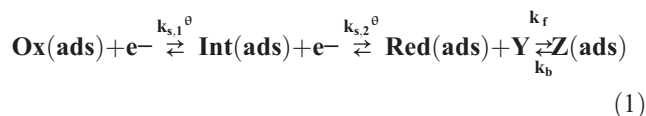
<sup>3</sup> Department of Inorganic and Analytical Chemistry, University of Lodz, Tamka 12, Łódź, Poland

54 for determination of thermodynamic and kinetic parameters  
 55 relevant to both electron transfers and the coupled chemical  
 56 reactions [11, 14–20].

57 When voltammetric peaks related to both electrode reac-  
 58 tion steps of a given redox enzyme are separated for at least  
 59 [150 mV], it is easily achievable to determine all relevant ki-  
 60 netic and thermodynamic parameters of the two redox steps  
 61 [11, 16–19]. However, if the two electron transfers take place  
 62 at the same potential, the overall electrode mechanism is as-  
 63 sociated with a SW voltammogram featuring single oxidation-  
 64 reduction voltammetric pattern. Under such conditions, it is  
 65 quite difficult to recognize whether the existing peak is due to  
 66 a single two-electron transfer step, or it is a consequence of  
 67 two, successive one-electron electrode transformations.  
 68 Hence, in the current work, we focus on developing an ap-  
 69 proach in SWV to recognize a two-step successive surface  
 70 electrode mechanism, under conditions where both electron  
 71 transfer steps occur at the same potential. The methodology  
 72 presented could help researchers working in enzymatic elec-  
 73 trochemistry to design proper voltammetric experiments for  
 74 recognizing particular two-step surface electrode reaction. To  
 75 the best of our knowledge, the methodology presented in this  
 76 work has not been considered so far in the theory of square-  
 77 wave voltammetry of two-step electrode mechanisms  
 78 [11–20]. It is finally worth mentioning that the current study  
 79 is also adequate to analyse the so-called “surface electrode  
 80 mechanisms” [21–24], i.e. electrode reactions taking place  
 81 exclusively from an adsorbed state.

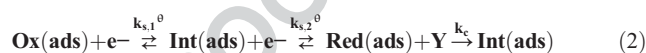
## 82 Details of theoretical models

83 Electrode mechanisms consisting of two successive elec-  
 84 tron transfers, coupled with a follow-up chemical reaction  
 85 to the second electrode step, are analyzed under condi-  
 86 tions of protein-film square-wave voltammetry. The first  
 87 mechanism is the so-called “surface EECrev”, while the  
 88 second one is “surface EEC’ catalytic” mechanism. In the  
 89 abbreviation for the “surface EECrev mechanism”, the  
 90 term “E” describes the electron transfer step, while  
 91 “Crev” refers to a reversible chemical reaction. In the  
 92 surface EEC’ mechanism, the symbol C’ stands for a re-  
 93 generative chemical reaction. In both mechanisms, we  
 94 consider an enzymatic electrode transformation with all  
 95 species firmly immobilized on the surface of the working  
 96 electrode. The electrode transformation of the initial en-  
 97 zymatic form Ox(ads) to the final redox form Red(ads) in  
 98 both mechanisms occurs in two successive one-electron  
 99 steps. In mechanism (1), we assume that the final enzy-  
 100 matic product (Red(ads)) undergoes follow-up reversible  
 101 chemical reaction with an electrochemically inactive sub-  
 102 strate “Y”. Schematic representation of such process  
 103 (mechanism (1)) is as follows:



106 Only enzymatic species Ox(ads) are present on the electrode surface at the  
 107 beginning of the experiment. In a first approximation, it has been assumed that  
 108 all immobilized species are uniformly adsorbed (“ads”) without any lateral  
 109 interactions. With Int(ads), we assign electroactive enzymatic species formed  
 110 as an intermediate in the first electrode reduction step. With Red(ads), we  
 111 assign the final redox-active enzymatic species, generated electrochemically  
 112 during the second electrode transfer step from Int(ads). With “Y”, we define  
 113 species present in the electrochemical cell that show no electrochemical activ-  
 114 ity in the potential region used for the voltammetric experiment. Y is supposed  
 115 to react in a selective and chemically reversible fashion with Red(ads) species,  
 116 converting them to the final electrochemically inactive product Z (ads)  
 117 (reaction Eq. 1).  
 118

119 The second electrode mechanism considered is the so-called “surface cata-  
 120 lytic EEC’ mechanism”, also known as a “surface regenerative EEC’ mecha-  
 121 nism”, which can be described with reaction Eq. (2):



124 The major difference between mechanisms (1) and (2) is  
 125 seen in the nature of the chemical reaction. Indeed, in mech-  
 126 anism (2), it is assumed that the electrochemically inactive  
 127 reactant “Y” irreversibly reacts with Red(ads), in a way to  
 128 regenerate the intermediate Int(ads). In both mechanisms, we  
 129 assume that the “Y” substrate is present in a large excess in the  
 130 electrochemical cell. Therefore, we assume that the concen-  
 131 tration of “Y” is constant on the electrode surface in the course  
 132 of the voltammetric experiment. Consequently, the chemical  
 133 steps in both mechanisms are assumed to be of a pseudo-first  
 134 order in terms of chemical kinetics.  
 135

136 Both mechanisms are solved under the following boundary  
 137 conditions:

$$t = 0; \Gamma(\text{Ox}) = \Gamma^*(\text{Ox}); \Gamma(\text{Int}) + \Gamma(\text{Red}) + \Gamma(\text{Z}) = 0$$

For  $t > 0$ , the following conditions apply:

$$t > 0; \Gamma(\text{Ox}) + \Gamma(\text{Int}) + \Gamma(\text{Red}) + \Gamma(\text{Z}) = \Gamma^*(\text{Ox}) \quad (\text{for mechanism 1})$$

$$t > 0; \Gamma(\text{Ox}) + \Gamma(\text{Int}) + \Gamma(\text{Red}) = \Gamma^*(\text{Ox}) \quad (\text{for mechanism 2})$$

$$d\Gamma(\text{Ox})/dt = -I_1/(FS) \quad (\text{for mechanisms 1 and 2})$$

$$d\Gamma(\text{Int})/dt = I_1/(FS) - I_2/(FS) \quad (\text{for mechanisms 1 and 2})$$

$$d\Gamma(\text{Red})/dt = I_2/(FS) - k_f\Gamma(\text{Red}) + k_b\Gamma(\text{Z}) \quad (\text{for mechanism 1})$$

$$d\Gamma(\text{Int})/dt = I_1/(FS) - I_2/(FS) + k_c\Gamma(\text{Red}) \quad (\text{for mechanism 2})$$

$$d\Gamma(\text{Red})/dt = I_2/(FS) - k_c\Gamma(\text{Red}) \quad (\text{for mechanism 2})$$

157 In both models, we assume that Butler-Volmer formalism  
 158 applies for the interdependence of the electric potential ( $E$ ),  
 159 the current ( $I$ ), the electrode reaction kinetic parameters (i.e.  
 160 the standard rate constant  $k_s^*$  and electron transfer coefficient

161  $\alpha$ ) and the surface concentration  $\Gamma$ . The analytical solutions of  
 162 electrode mechanisms (1) and (2) are given in [11, 17], respec-  
 163 tively. In [17], a detailed MATHCAD file containing all recur-  
 164 rent formulas for calculating SW voltammograms of the sur-  
 165 face EECrev mechanism is provided.

166 In both mechanisms, we consider reduction currents as  
 167 positive, and negative sign is ascribed to oxidation currents.  
 168 All theoretical voltammograms are presented versus the for-  
 169 mal potential of the first electrode process (assigned as a “peak  
 170 I”).

171 **Critical parameters controlling voltammetric**  
 172 **behaviour**

173 Dimensionless current  $\Psi$  of calculated voltammograms for  
 174 both mechanisms is defined as a sum of partial currents related  
 175 to the first ( $\Psi_I$ ) and the second ( $\Psi_{II}$ ) electrode step:  $\Psi = \Psi_I + \Psi_{II}$ .  
 176 Each dimensionless current, related to the corresponding elec-  
 177 tron transfer step, is normalized as follows:  $\Psi_I = I_1/[FS\Gamma$   
 178  $(Ox)^*]$  and  $\Psi_{II} = I_2/[FS\Gamma(Ox)]$ . Here,  $S$  is the active surface  
 179 area of working electrode and  $f$  is the frequency of SW pulses  
 180 defined as  $f = 1/(2t_p)$ , where  $t_p$  is the duration time of a single  
 181 potential pulse in SWV.  $\Gamma(Ox)^*$  stands for the total surface  
 182 concentration, which corresponds to the surface concentration  
 183 of the initially adsorbed Ox(ads) species. The potential driving  
 184 force of each electrode reactions defined in a form of a dimen-  
 185 sionless potentials is:  $\Phi_1 = F(E - E_1^\ominus)/RT$  and  $\Phi_2 = F(E - E_2^\ominus)/$   
 186  $RT$ , where  $E_1^\ominus$  and  $E_2^\ominus$  are the standard redox potential of the  
 187 first and second electrode steps, respectively.  $T$  is symbol of  
 188 the thermodynamic temperature (it was set to 298 K in all  
 189 simulations),  $R$  is universal gas constant and  $F$  is the  
 190 Faraday constant.

191 Features of simulated SW voltammetric patterns depend on  
 192 several dimensionless parameters as follows. (a) The dimen-  
 193 sionless electrode kinetic parameters related to each electron  
 194 transfers:  $KI = k_{s,1}^\ominus/f$  and  $KII = k_{s,2}^\ominus/f$ . Both  $KI$  and  $KII$  reflect  
 195 the influence of the electrode kinetics represented by the stan-  
 196 dard rate constants ( $k_{s,1}^\ominus$  and  $k_{s,2}^\ominus$ ) relative to the critical time  
 197 window of the experiment (i.e. SW frequency,  $f$ ).

198 (b) For the surface EECrev mechanism, dimensionless  
 199 chemical parameter  $K_{chemical} = \varepsilon/f$  affects the features of SW  
 200 voltammograms. In the last equation,  $\varepsilon$  is the cumulative rate  
 201 constant  $\varepsilon = (k_f + k_b)$ , where  $k_f$  and  $k_b$  are the rate constants of  
 202 the forward and backward chemical reaction, respectively.  
 203 Hence, the dimensionless parameter  $K_{chemical}$  reflects the ef-  
 204 fect of the chemical kinetics, relative to the time widow of the  
 205 SW experiment. In addition, mechanism (1) is affected by the  
 206 equilibrium constant defined as  $K_{eq} = k_f/k_b$ .

207 (c) For the surface catalytic EEC' mechanism, the dimen-  
 208 sionless chemical kinetic parameter is defined as  $K_{catalytic} = k_c/$   
 209  $f$ . In last equation,  $k_c$  is the rate constant of the regenerative  
 210 (catalytic) chemical reaction. At this stage, it is worth to

emphasize that both chemical parameters related to the chem- 211  
 ical steps ( $\varepsilon$  and  $k_c$ ) are of pseudo-first order. Both,  $\varepsilon$  and  $k_c$ , 212  
 depend on the concentration of substrate “Y” as follows:  $\varepsilon =$  213  
 $[k_f^\ominus c(Y) + k_b]$  for the mechanism (1) and  $k_c = k_c^\ominus c(Y)$  for the 214  
 mechanism (2). In the last equations,  $k_f^\ominus$  and  $k_c^\ominus$  are real, 215  
 second-order chemical rate constants, while  $c(Y)$  is the molar 216  
 concentration of the substrate Y, which remains constant in the 217  
 course of the experiment. 218

219 The parameters of applied potential in all calculations were 219  
 set to: SW frequency  $f = 10$  Hz, SW amplitude  $E_{sw} = 50$  mV, 220  
 and potential step  $dE = 4$  mV. In addition, electron transfer 221  
 coefficient to both electron transfer steps and both mecha- 222  
 nisms was set to  $\alpha = 0.5$ . The net SWV current at all voltam- 223  
 mograms is represented by black colour, while blue colour is 224  
 associated to the forward (reduction) currents. Red colour is 225  
 associated to the backward currents of all calculated 226  
 voltammograms. 227

228 **Results and discussions**

229 In previous works, we have presented comprehensive theoret- 229  
 ical studies of the surface EE, ECE, EECirr, EECrev and EEC' 230  
 mechanisms [11–20] under conditions of SWV. In [11, 17, 231  
 18], a set of relevant theoretical voltammetric features of the 232  
 surface EECrev, EEC' and EECirr systems have been elabo- 233  
 rated, respectively. A scenario for appearance of two SW 234  
 peaks, separated for at least 150 mV (in absolute value), has 235  
 been comprehensively analyzed for the surface EECirr, 236  
 EECrev and EEC' mechanisms [11]. In order to understand 237  
 voltammetric characteristics of the present EECrev mecha- 238  
 nism when the formal potentials of the two-electron transfer 239  
 steps are identical, we briefly recall a small segment of this 240  
 mechanism under conditions when the two electrode reactions 241  
 are separated in their formal redox potentials. 242

243 SW voltammograms calculated for potential difference of 243  
 $-300$  mV between the second and the first electron transfer 244  
 step are shown in Fig. 1. The figure depicts the effect of the 245  
 dimensionless chemical rate parameter  $K_{chemical}$  calculated for 246  
 $Keq = 1$ ,  $KI = 1.5$  and  $KII = 1.78$ . Since the rate of the chemi- 247  
 cal step affects directly the second electron transfer, one wit- 248  
 nesses remarkable changes of peak II (positioned at more nega- 249  
 tive potentials) caused by the increasing of  $K_{chemical}$ . As the 250  
 magnitude of  $K_{chemical}$  increases from 0.001 to 0.1, the inten- 251  
 sity of all current components of the second process signifi- 252  
 cantly diminishes. At the same time, the net peak potential of 253  
 the second peak shifts for  $59$  mV/ $n$  in a positive direction by a 254  
 tenfold increase of  $K_{chemical}$ . 255

256 For  $Keq \leq 1$ , one observes very specific phenomenon; in- 256  
 deed, the dependence of the net peak current  $\Psi_{netp,II}$  on the 257  
 electrode kinetic parameter  $KII$  features well-developed max- 258  
 imum, the position of which is a function of  $K_{chemical}$  (Fig. 2). 259  
 As elaborated in [21, 22], this specific dependence known as a 260



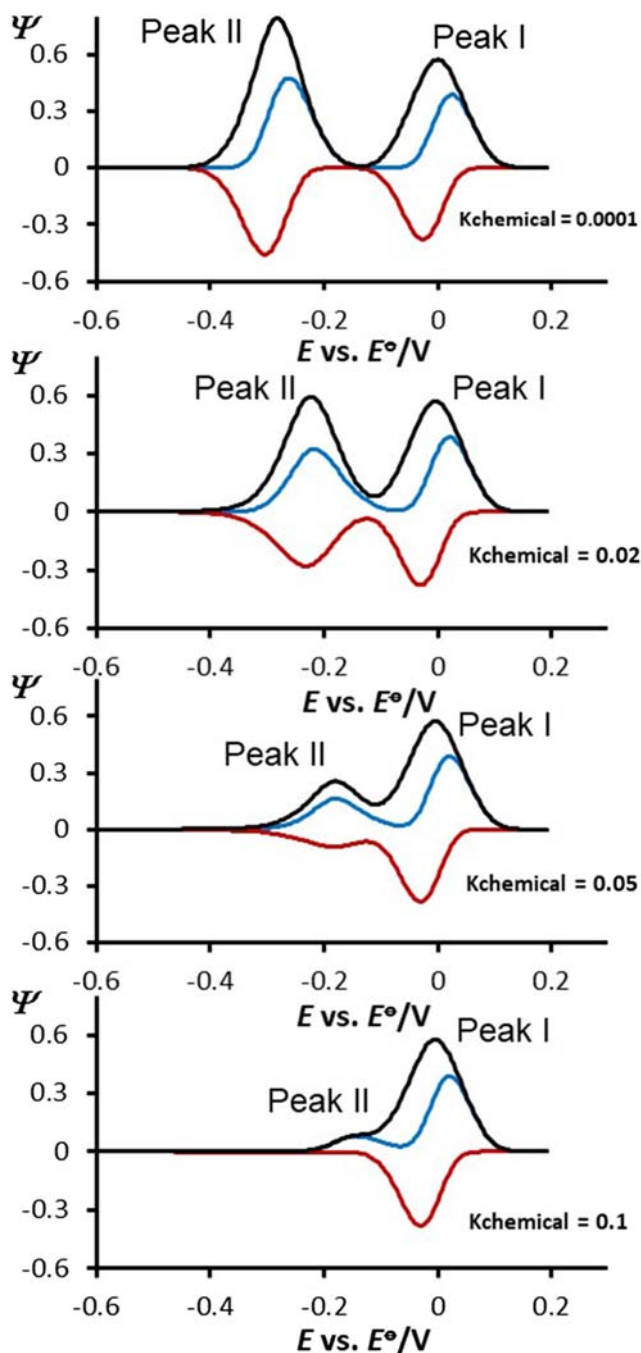


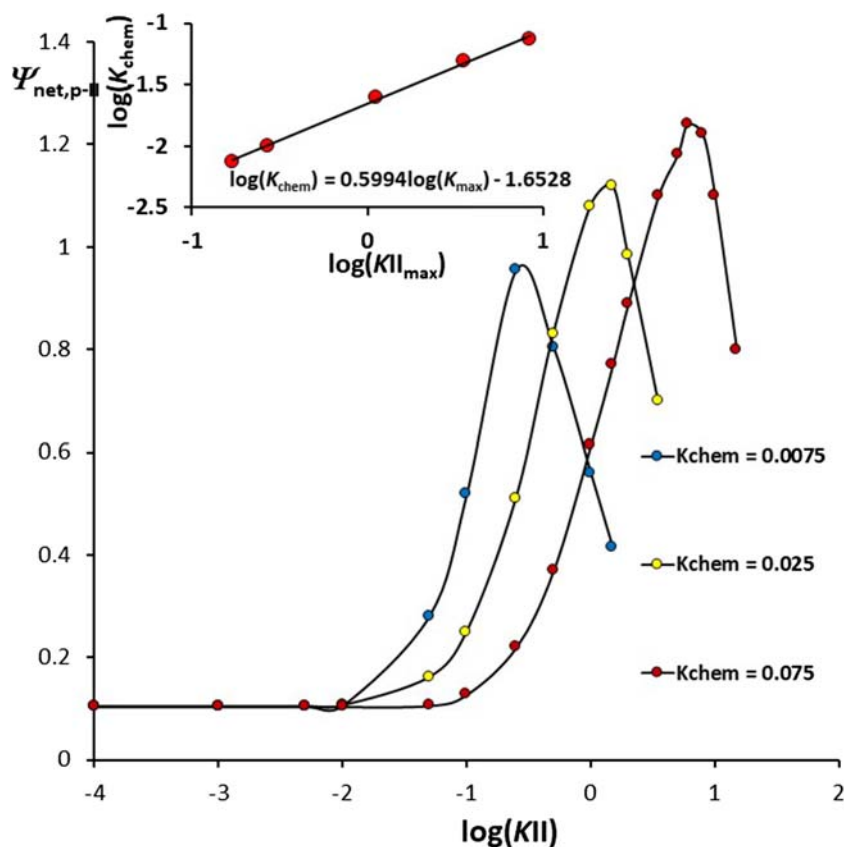
**Fig. 1** Surface EECrev mechanism: square-wave voltammograms simulated for a potential separation of  $-300$  mV between the second and the first electron transfer step. Voltammetric patterns reflect the effect of the chemical rate parameter  $K_{\text{chemical}}$ . The values of  $K_{\text{chemical}}$  are given in the charts. In the simulations, the value of the kinetic of electron transfer of the first electron transfer step was  $K_{\text{I}} = 1.50$ , while  $K_{\text{II}} = 1.78$ . The value of the equilibrium constant of the chemical reaction was set to  $K_{\text{eq}} = 1$ . Other simulation parameters were SW frequency  $f = 10$  Hz, SW amplitude  $E_{\text{sw}} = 50$  mV, potential step  $dE = 4$  mV and temperature  $T = 298$  K. In all simulations, the electron transfer coefficients of the first and second electrode reaction were set to the same value of  $\alpha = 0.5$ . The stoichiometric number of electrons exchanged was  $n_1 = n_2 = 1$

“quasireversible maximum” appears in all surface mechanisms. The quasireversible maximum of the surface EECrev mechanism is a consequence of the chronoamperometric properties of the system and the current sampling procedure applied in SWV. Important part of this behaviour is also ascribed to variation of the surface concentration of Red(ads) species with time in the so-called “dead time” of SW potential pulses [24], i.e. in the course of the pulse when the current is not sampled. In [11, 19, 20], a method has been proposed for estimation of the chemical parameter  $K_{\text{chemical}}$  by means of the linear function presented in Fig. 2, which represents the functional relationship of the maximum position versus the rate of the chemical reaction.

It is useful to recall that the rate of the follow-up chemical reaction causes even more complex effect to the voltammetric patterns of the surface EECrev mechanism when the electron transfer step is very fast. As elaborated in [21–24], a representative feature of all “fast” surface electrode mechanisms is the “splitting of the net SW peak” (see Fig. 3a). Under such conditions, when peak II and peak I are separated for at least  $-200$  mV, an increase of the chemical reaction rate (i.e.  $K_{\text{chemical}} > 0.001$ ) produces simultaneous increase of all current components of the peak II (Fig. 3b–d), contrary to the reasonable expectation the response to diminish. For  $K_{\text{chemical}} > 0.01$ , the net peak splitting vanishes (Fig. 3c), while the magnitude of both forward (reductive) and backward (oxidative) SW components increases for about 200 times (compare Fig. 3d with a). Eventually, for  $K_{\text{chemical}} > 0.06$ , all peak currents of the second process start diminishing, while peak II shifts to more positive potentials, as expected for an EECrev mechanism (Fig. 3e, f).

The origin of such specific and peculiar voltammetric behaviour is elaborated in more details in [19, 20, 24]. Briefly, fast electron transfer reaction coupled to chemical reactions having moderate-to-fast kinetics leads to formation of a significant amount of Red(ads) species at the beginning of a potential pulse (i.e. in the non-current measuring time segments) [24]. In the course of the pulse, the redox species approaches rapidly to redox equilibrium when the electrode reaction is fast. Thus, small current remains to be sampled at the end of the potential pulse. However, in the presence of a follow-up chemical reaction, the redox equilibrium cannot be established, causing the redox transformations to proceed significantly even at the end of the potential pulse when the current is being sampled. Consequently, both forward and backward SW components significantly increase by increasing the rate of the follow-up chemical reaction, while the splitting of the net peak vanishes [19, 20, 24]. As reported in [11, 19, 20], these voltammetric features can be exploited for evaluation of the kinetic and thermodynamic parameters of the second electrochemical step and the follow-up chemical reaction of the overall EECrev mechanism (cf. Figs. 1, 2 and 3).

**Fig. 2** Surface EECrev mechanism: a series of quasireversible maxima calculated for  $Keq = 10$  for different rates of the chemical reaction. The calculated patterns correspond to the second SW voltammetric peak (peak II) positioned at more negative potentials. The inset shows the relationship between  $\log(K_{\text{chemical}})$  and the logarithm of the electrode kinetic parameter  $\log(K_{II_{\text{max}}})$  associated to the position of the quasireversible maximum. All other simulation parameters were the same as for Fig. 1



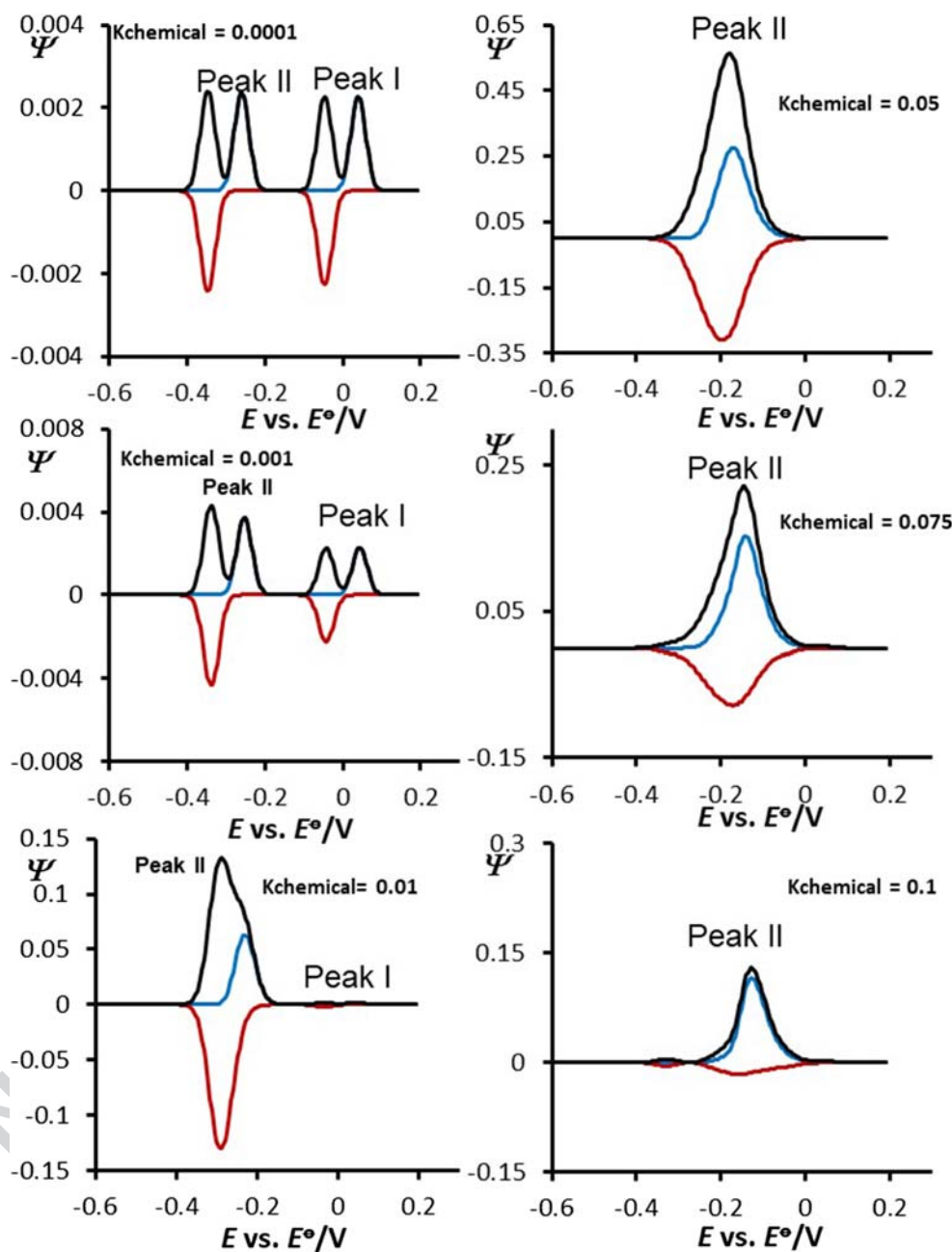
314 As briefly mentioned in the “Introduction” section, the  
 315 most challenging situation for all two-step successive mecha-  
 316 nisms is to characterize the two-electron transfer steps when  
 317 they occur at the same potential. Under such circumstances,  
 318 one observes SW voltammograms consisting of a single  
 319 oxidation-reduction pattern, which “hides” features of both  
 320 electron transfer steps (Fig. 4a). In such scenario, the major  
 321 goal is to reveal whether the single voltammetric peak is due  
 322 to a single, simultaneous two-electron transfer process, or it is  
 323 a consequence of two successive one-electron transfer steps.  
 324 Every misinterpretation of the “diagnosed” mechanism might  
 325 lead to erroneous estimation of kinetic and thermodynamic  
 326 parameters.

327 The first goal in such scenario is to find simple, qualitative  
 328 criterion for recognizing the EECrev mechanism when the  
 329 two-electron transfer steps are characterized with the same  
 330 formal potential. The effect of the dimensionless chemical  
 331 parameter  $K_{\text{chemical}}$  to the voltammetric patterns is shown in  
 332 Fig. 4. SW voltammograms are simulated for  $Keq = 0.1$ , and  
 333 electrode kinetic parameters  $KI = 1.26$  and  $KII = 2.82$ .  
 334 Following the discussions of the data presented in Figs. 1  
 335 and 3, and bearing in mind the features of the simple surface  
 336 EC mechanism as a function  $K_{\text{chemical}}$  [11, 19, 20], one expects  
 337 separation of both overlapped electron transfer steps to occur  
 338 by increasing the rate of the follow-up chemical reaction. It is  
 339 plausible to expect the kinetics of the chemical reaction to

340 affect mainly voltammetric features of the second electron  
 341 transfer (peak II). As presented in Figs. 1 and 3, an increase  
 342 of the chemical reaction rate (expressed via  $K_{\text{chemical}}$ ) shifts the  
 343 second electron transfer process towards more positive poten-  
 344 tials. Such scenario in Fig. 4 occurs for  $K_{\text{chemical}} > 0.02$  (Fig.  
 345 4b). For  $K_{\text{chemical}} > 0.05$  (Fig. 4d), one observes two well-  
 346 separated processes: one at potential of 0.0 V (peak I), as-  
 347 cribed to the first electron transfer, and the second peak at  
 348 about +0.15 V (peak II), associated to the second electron  
 349 transfer step. Once the two processes are separated for at least  
 350 150 mV (Fig. 4d, e), one can apply the methodology for esti-  
 351 mation of the kinetic parameters as elaborated in [11, 19–24].

352 Another interesting scenario is met in situation when both  
 353 electron transfer steps of a surface EECrev mechanism are  
 354 very fast, while taking place at the same formal potential.  
 355 Under such conditions, one observes a single, split net SW  
 356 peak (Fig. 5a). Again, via altering the value of  $K_{\text{chemical}}$ , one  
 357 can achieve well separation between the two electron trans-  
 358 fers, as represented in Fig. 5b–f. By increasing the magnitude  
 359 of  $K_{\text{chemical}}$ , one can get a voltammetric pattern consisting of a  
 360 “split SW net peak” that is related to the first electron transfer  
 361 step (peak I), and a single net peak displaced to more positive  
 362 potentials, which is associated to the second electron transfer  
 363 that is coupled with the chemical reaction (peak II) (see Fig.  
 364 5e, f). From the voltammetric patterns (cf. Fig. 5e, f), one can  
 365 estimate the values of  $KI$ ,  $KII$ ,  $K_{\text{chemical}}$  and  $Keq$ . For the

**Fig. 3** Surface EEC<sub>rev</sub> mechanism: square-wave voltammograms calculated for a potential difference of  $-300$  mV between the second and the first electron transfer step. The voltammograms show the effect of the chemical rate parameter  $K_{\text{chemical}}$  in the region of fast electron transfers of both steps ( $K_{\text{I}} = 10$  and  $K_{\text{II}} = 10$ ). The values of  $K_{\text{chemical}}$  are given in the charts. Value of the equilibrium constant of chemical reaction was set to  $K_{\text{eq}} = 1000$ . Other simulation parameters were the same as for Fig. 1



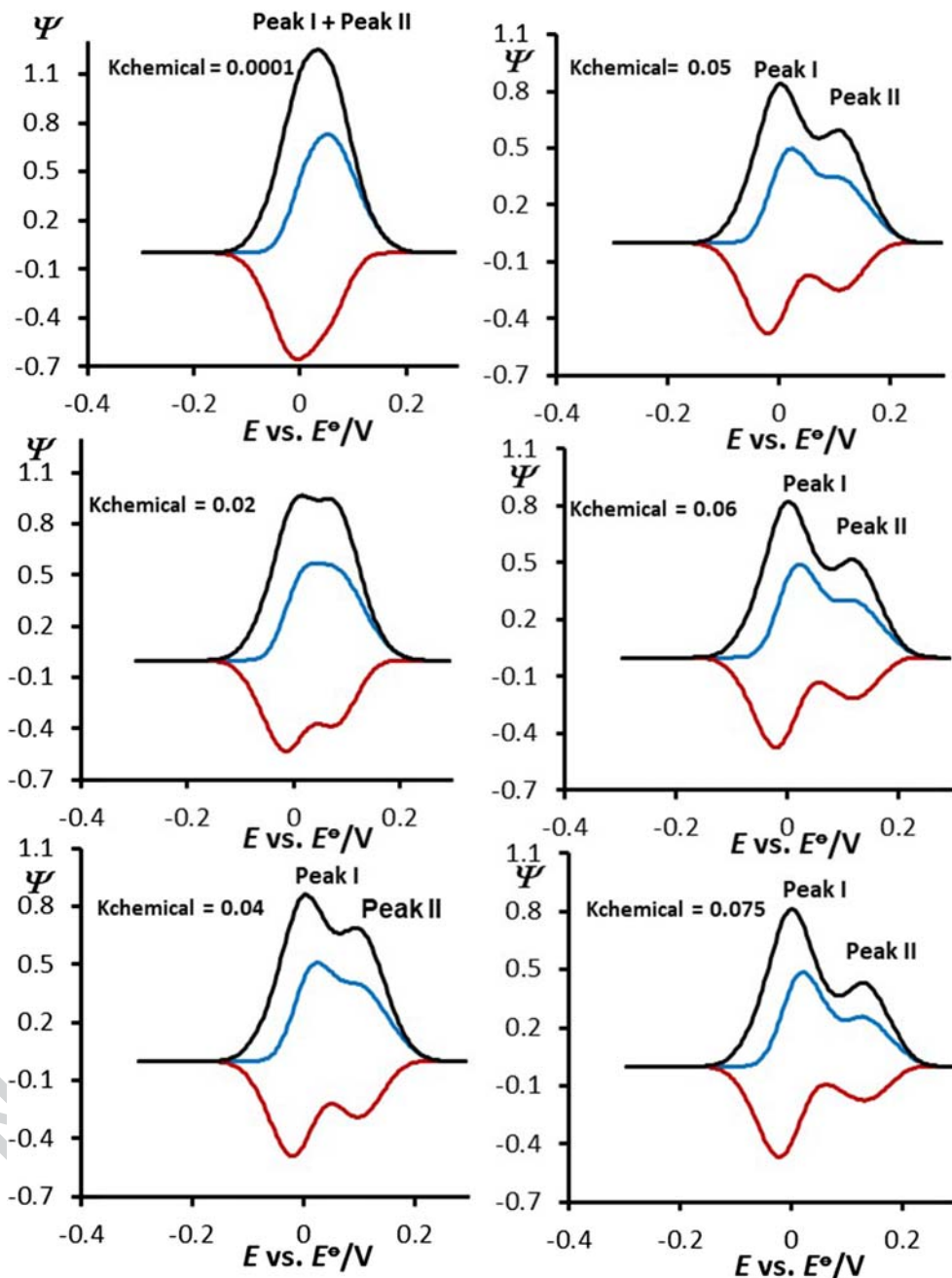
366 determination of  $K_{\text{I}}$  (peak I), one can use the method of “split  
 367 net peak” [21, 23], while for determination of  $K_{\text{II}}$ ,  $K_{\text{chemical}}$   
 368 and  $K_{\text{eq}}$ , one can utilize the methodology elaborated in  
 369 [19–21, 24].

370 From the voltammograms presented in Figs. 4 and 5,  
 371 we recognize that the kinetics of the follow-up chemical  
 372 reaction coupled to the second electron transfer might lead to a  
 373 successful separation of two consecutive electron transfer  
 374 steps, when these occur at the same potential. Theoretically  
 375 speaking, one expects differentiation of the two-electron  
 376 transfer steps to be possible for the EEC' catalytic mechanism as  
 377 well. As shown in Fig. 6, an increase of the catalytic rate

378 parameter  $K_{\text{catalytic}}$  leads to the displacement of the second  
 379 SWV peak to more negative potentials (see Fig. 6b–d), which  
 380 is in agreement with previous data [11, 17, 25]. However,  
 381 referring to voltammograms (Fig. 6b–d), it can be seen that  
 382 the rate of the regenerative chemical reaction starts affecting  
 383 the ascending branch of net peak at rather positive potentials.  
 384 Consequently, the obtained catalytic current overlaps  
 385 completely the response of the first electron transfer, which  
 386 becomes completely invisible at higher rates of the regenerative  
 387 reaction.

388 Voltammograms a'–d' in Fig. 6 are assigned to the first  
 389 electron transfer step (peak I), being extracted out of the

**Fig. 4** Surface EEC<sub>rev</sub> mechanism: effect of the chemical rate parameter  $K_{\text{chemical}}$  to the voltammetric patterns, calculated when both electron transfers take place at the same potential. Voltammograms are simulated in the region of moderate rates of the electron transfer of both steps, i.e.  $K_{\text{I}} = 1.26$  and  $K_{\text{II}} = 2.82$ . The values of  $K_{\text{chemical}}$  are given in the charts. Value of the equilibrium constant of chemical reaction was set to  $K_{\text{eq}} = 0.1$ . Other simulation parameters were the same as for Fig. 1



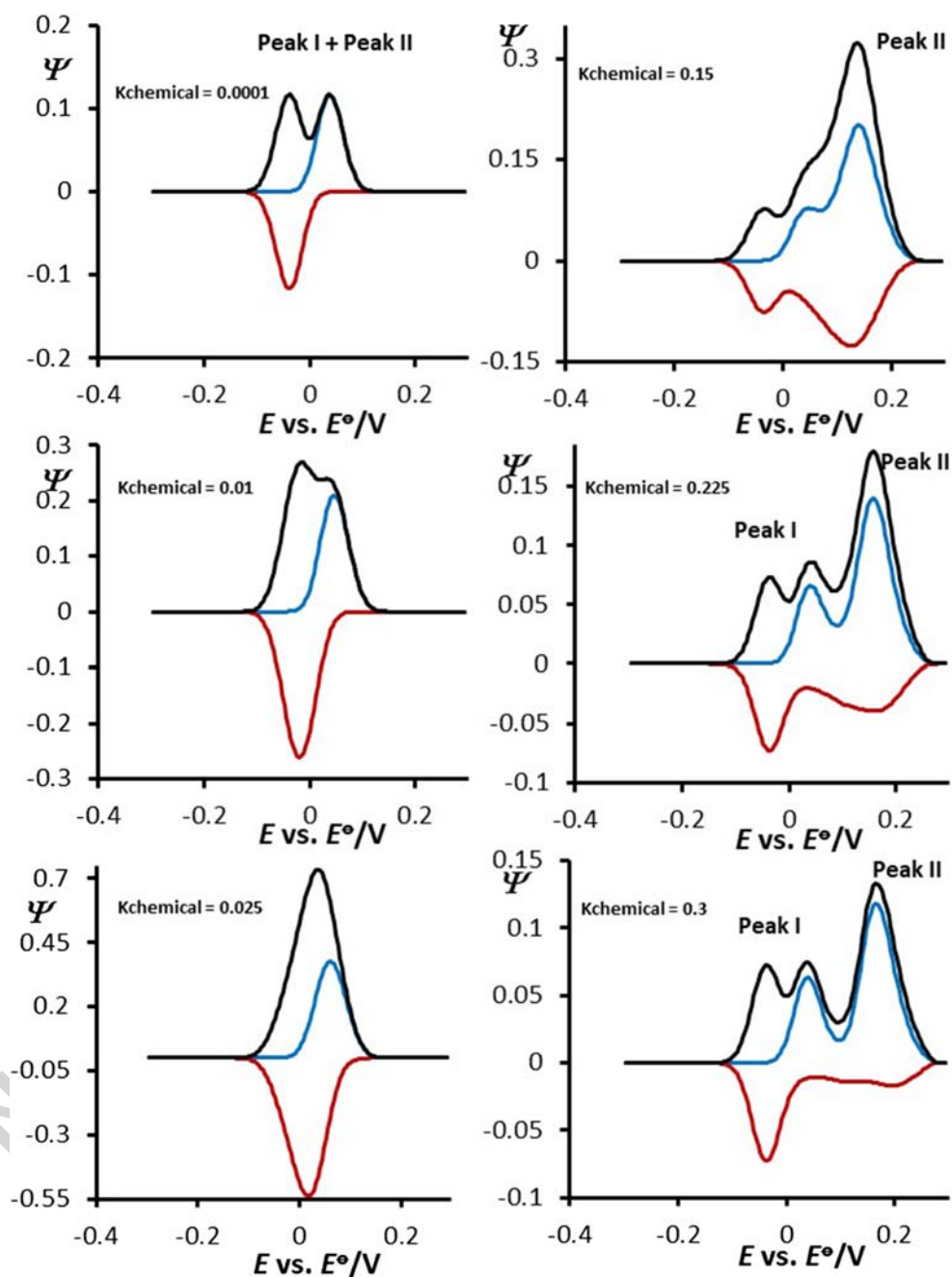
390 overall voltammograms Fig. 6a–d. The arrows show the position where peak I should appear in the overall voltammetric  
 391 response. Because peak I is associated with peak II, we observe that peak I gets also slightly affected by  $K_{\text{catalytic}}$ . Its  
 392 position shifts for 50 mV in a negative direction by increasing of  $K_{\text{catalytic}}$  from 0.0001 to 0.04, while its height gets unaffected  
 393 at  $K_{\text{catalytic}} > 0.04$ . Unfortunately, the intensive catalytic current does not allow exploring the features of the separate  
 394 electron transfer steps of the EEC' mechanism. This means that only via the features of the surface EEC<sub>rev</sub> mechanism,  
 395 as elaborated in Figs. 4 and 5, one can achieve efficient separation and characterization of the two-electron transfer steps.  
 396  
 397  
 398  
 399  
 400  
 401

**Conclusions**

Lipophilic enzymes containing multivalent ions or quinone  
 403 moieties as redox-active centres are ubiquitous, while playing  
 404 a crucial role in many cellular reactions. In the living systems,  
 405 these enzymes can be turned into redox inactive state via  
 406 follow-up chemical reaction [26]. The inactivation of many  
 407 enzymes can provide important data about chemistry of the  
 408 enzyme's active sites and on the catalytic potential. The elec-  
 409 trochemical transformation of such enzymes commonly fol-  
 410 lows a pathway of successive electron transfers in two steps. If  
 411 both electron transfer steps in such systems occur at the same  
 412



**Fig. 5** Surface EECrev mechanism: effect of the chemical rate parameter  $K_{\text{chemical}}$ . All voltammetric patterns are calculated when both electron transfers take place as the same potential, in the region of fast rate of the electron transfer of both steps, i.e.  $K_{\text{I}} = 5$  and  $K_{\text{II}} = 5$ . The values of  $K_{\text{chemical}}$  are given in the charts. Value of the equilibrium constant of chemical reaction was set to  $K_{\text{eq}} = 100$ . Other simulation parameters were the same as for Fig. 1

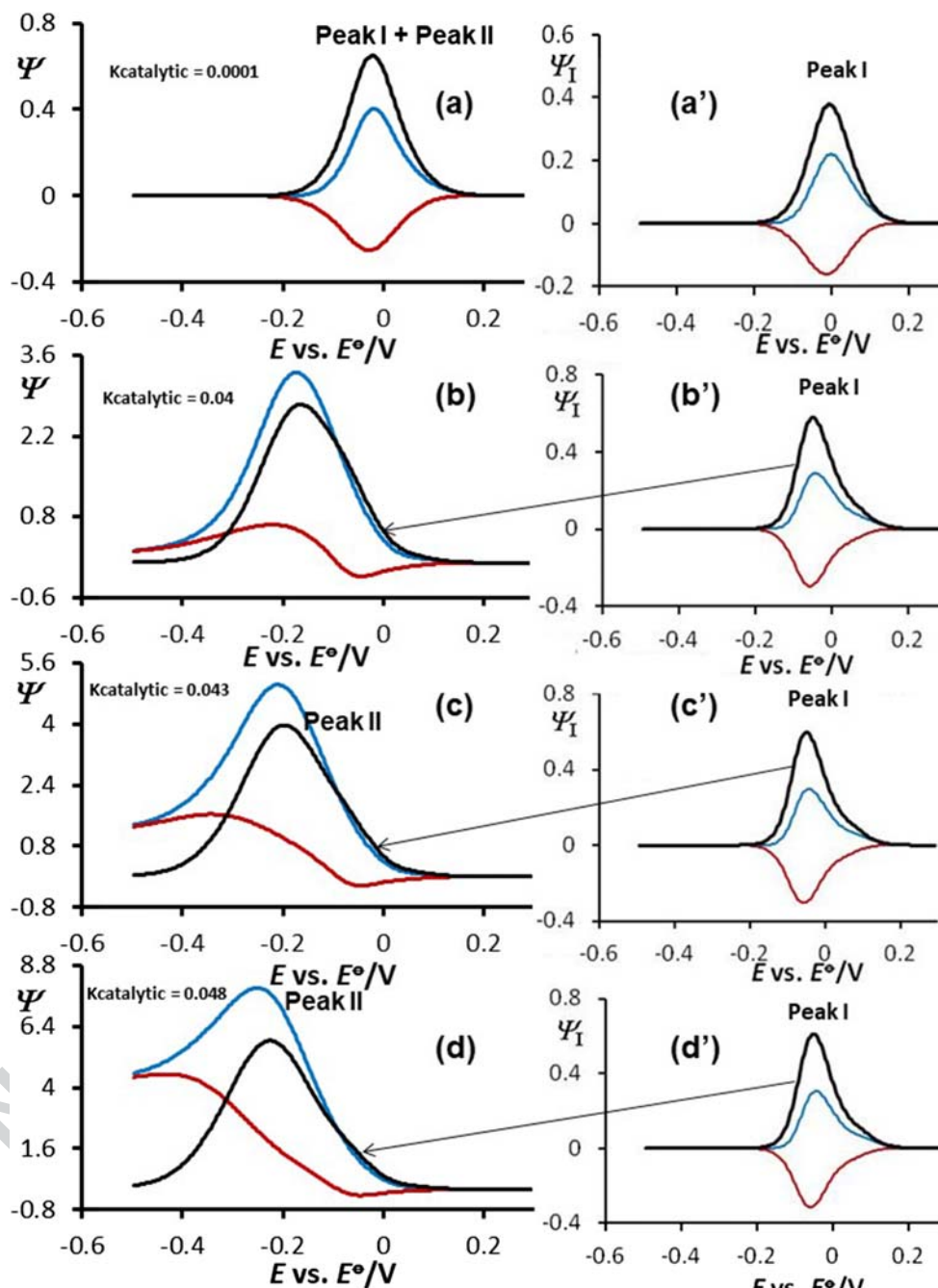


413 potential, the electrochemistry of this class of enzymes will be  
 414 portrayed in a single oxidation-reduction pattern when analyzed in “protein-film voltammetry”. The single square-  
 415 wave voltammogram, obtained under defined circumstances, will “hide” in its shape the features of both electron transfer  
 416 steps. If this happens, a challenging task is to recognize the nature of electrode mechanism encountered in the analyzed  
 417 system. In this work, we focused on developing efficient method to evaluate the two-step electrode mechanism, when  
 418 both steps take place at same potential, by exploring the features of surface EECrev mechanism in SWV. As elaborated in  
 419 this work, increased rate of the follow-up chemical reaction,  
 420  
 421  
 422  
 423  
 424

expressed via  $K_{\text{chemical}}$ , displaces the second electron transfer  
 process of a surface EECrev mechanism towards more positive  
 potentials. Consequently, one can explore this feature to  
 separate the two EE steps, if both happen at the same potential.  
 If we recall that the dimensionless chemical rate parameter  
 $K_{\text{chemical}}$  in surface EECrev mechanism is defined as  
 $K_{\text{chemical}} = [k_{\text{f}}^{\text{c}}c(\text{Y}) + k_{\text{b}}]/f$ , we recognize that modification  
 of magnitude of  $K_{\text{chemical}}$  can be achieved in two ways: (a)  
 via altering the SW frequency  $f$  and (b) via altering the con-  
 centration of substrate Y. Because the SW frequency affects  
 simultaneously the rates of electron transfer of both steps (via  
 $K_{\text{I}}$  and  $K_{\text{II}}$ ) and the magnitude of dimensionless chemical  
 425  
 426  
 427  
 428  
 429  
 430  
 431  
 432  
 433  
 434  
 435  
 436



**Fig. 6** Surface EEC' catalytic mechanism: **a–d** Effect of the catalytic rate parameter  $K_{\text{catalytic}}$ . All voltammetric patterns are calculated when both electron transfers take place at the same potential, in the region of slow rate of the electron transfer of both steps, i.e.  $K_{\text{I}} = 0.2$  and  $K_{\text{II}} = 0.2$ . The values of  $K_{\text{catalytic}}$  are given in the charts. The panels (a'–d') correspond to the currents of peak I, extracted from the net SW voltammograms **a–d**. Other simulation parameters were the same as for Fig. 1



437 parameter  $K_{\text{chemical}}$ , altering the SW frequency will produce  
 438 complex voltammetric outputs. Therefore, in order to obtain  
 439 voltammetric patterns that will enable separation of the two  
 440 EE processes happening at same potential, modification of the  
 441 rate of chemical reaction should be achieved via modification  
 442 of the concentration of  $c(\text{Y})$ . It is important to mention that  
 443 these experiments in SWV should be performed at a constant  
 444 frequency. Once we get voltammograms with separated  
 445 peaks, as those presented in Figs. 4e and 5e, for example, then  
 446 we can apply suitable methodologies for thermodynamic and  
 447 kinetic evaluations related to both EE steps. For the

determination of the electron transfer coefficient  $\alpha$  of both 448  
 steps, one should explore the methodology elaborated in [27]. 449

**References**

450  
 451 1. Armstrong FA (2015) Electrifying metalloenzymes in: 451  
 metalloproteins: theory, calculations and experiments (Cho AE, 452  
 Goddar III WA, eds), CRC Press. Taylor&Francis Group, London 453  
 454 2. Leger C, Elliott SJ, Hoke KR, Jeuken LJC, Jones AK, Armstrong 454  
 FA (2003) Enzyme electrokinetics: using protein-film voltammetry 455

456 to investigate redox enzymes and their mechanism. *Biochem* 42: 498  
 457 8653–8662 499

458 3. Armstrong FA, Herring HA, Hirst J (1997) Reactions of complex 500  
 459 metalloproteins studied by protein-film voltammetry. *Chem Soc*  
 460 *Rev* 26:169 501

461 4. Armstrong FA (2002) Voltammetry of proteins. in: *Encyclopaedia*  
 462 *of electrochemistry* (Bard AJ, Stratmann M, Wilson GS, eds),  
 463 Wiley VCH, Weinheim 502

464 5. Jenner LP, Butt JN (2018) Electrochemistry of surface-confined 503  
 465 enzymes: inspiration, insight and opportunity for sustainable bio-  
 466 technology. *Curr Opin Electrochem* 8:81–88 504

467 6. Sies H, Parker L (2004) Quinones and quinone enzymes, in:  
 468 *methods in enzymology*. Academic Press, London 505

469 7. Kobayashi M, Shimizu S (1999) Cobalt proteins. *Eur J Biochem*  
 470 261(1):1–9 506

471 8. Hille R (2002) Molybdenum and tungsten in biology. *Trends*  
 472 *Biochem Sci* 27(7):360–367 507

473 9. Crans DC, Smeets JJ, Galdamauskas E, Yang L (2004) The chemistry  
 474 and biochemistry of vanadium and the biological activities exerted  
 475 by vanadium compounds. *Chem Rev* 104(2):849–902 508

476 10. Ermler U, Grabarse W, Shima S, Goubeaud M, Thauer RK (1998)  
 477 Active sites of transition-metal enzymes with focus on a nickel. 509  
 478 *Curr Opin Struct Biol* 8(6):749–758 510

479 11. Janeva M, Kokoskarova P, Maksimova V, Gulaboski R (2019)  
 480 Square-wave voltammetry of two-step surface redox mechanisms  
 481 coupled with chemical reactions—a theoretical overview. *Electroanal*  
 482 31:2488–2506 511

483 12. Gulaboski R, Mirceski V, Bogeski I, Hoth M (2012) Protein-film  
 484 voltammetry-electrochemical enzymatic spectroscopy: a review on  
 485 recent progress. *J Solid State Electrochem* 16:2315–2328 512

486 13. Gulaboski R, Kokoskarova P, Mitrev S (2012) Theoretical aspects  
 487 of several successive two-step redox mechanisms in protein-film  
 488 cyclic staircase voltammetry. *Electrochim Acta* 69:86–96 513

489 14. Mirceski V, Gulaboski R (2003) A theoretical and experimental  
 490 study of two-step quasireversible surface reaction by square-wave  
 491 voltammetry. *Croat Chem Acta* 76:37–48 514

492 15. Mirceski V, Gulaboski R, Lovric M, Bogeski I, Kappel R, Hoth M  
 493 (2013) Square-wave voltammetry: a review on recent progress.  
 494 *Electroanal* 25:2411–2422 515

495 16. Gulaboski R (2009) Surface ECE mechanism in protein-film volt-  
 496 ammetry—a theoretical study under conditions of square-wave volt-  
 497 ammetry. *J Solid State Electrochem* 13:1015–1024 516

17. Gulaboski R, Mihajlov L (2011) Catalytic mechanism in successive 498  
 two-step protein-film voltammetry—theoretical study in square- 499  
 wave voltammetry. *Biophys Chem* 155(1):1–9 500

18. Kokoskarova P, Maksimova V, Janeva M, Gulaboski R (2019) 501  
 Protein-film voltammetry of two-step electrode enzymatic reactions 502  
 coupled with an irreversible chemical reaction of a final product—a 503  
 theoretical study in square-wave voltammetry. *Electroanal* 31: 504  
 1454–1464 505

19. Gulaboski R, Janeva M, Maksimova V (2019) New aspects of 506  
 protein-film voltammetry of redox enzymes coupled to follow up 507  
 reversible chemical reaction in square-wave voltammetry. 508  
*Electroanal* 31:946–956 509

20. Gulaboski R, Mirceski V, Lovric M (2019) Square-wave protein- 510  
 film voltammetry: new insights in the enzymatic electrode process- 511  
 es coupled with chemical reactions. *J Solid State Electrochem* 23: 512  
 2493–2506 513

21. Mirceski V, Komorsky-Lovric S, Lovric M (2007) Square-wave 514  
 voltammetry, theory and application (Scholz F, ed.) Springer, 515  
 Berlin, Germany 516

22. Lovric M (2010) Square-wave voltammetry in electroanalytical 517  
 methods (Scholz F, ed.) Springer, Berlin, Germany, 2<sup>nd</sup> edition 518

23. Mirceski V, Lovric M (1997) Split square-wave voltammograms of 519  
 surface redox reactions. *Electroanal* 9:1283–1287 520

24. Gulaboski R (2019) Theoretical contribution towards understand- 521  
 ing specific behaviour of “simple” protein-film reactions in square- 522  
 wave voltammetry. *Electroanal* 31:545–553 523

25. Gulaboski R, Mirceski V (2015) New aspects of the 524  
 electrochemical-catalytic (EC<sup>+</sup>) mechanism in square-wave volt- 525  
 ammetry. *Electrochim Acta* 167:219–225 526

26. del Barrio M, Fourmond V (2019) Redox (in) activations of 527  
 metalloenzymes: a protein film voltammetry approach. 528  
*ChemElectroChem* 6:4949–4962 529

27. Gulaboski R, Lovric M, Mirceski V, Bogeski I (2008) A new rapid 530  
 and simple method to determine the kinetics of electrode reactions 531  
 of biologically relevant compounds from the half-peak width of the 532  
 square-wave voltammograms. *Biophys Chem* 138(3):130–137 533

**Publisher's note** Springer Nature remains neutral with regard to jurisdic- 534  
 tional claims in published maps and institutional affiliations. 535

AUTHOR QUERY

**AUTHOR PLEASE ANSWER QUERY.**

Q1. Please check if the affiliations are presented correctly.

UNCORRECTED PROOF